

# FINAL DESIGN REPORT: FUSELAGE

*Harsha Pandey, Ushasree Perakalapudi, Siddardth Pathipaka, Abhishek Iyer*

*University of Illinois, Urbana-Champaign*

The report presents the design and analysis of a composite fuselage section. The fuselage design adheres to specific constraints as laid out in the guidelines. Through theoretical calculations and simulations is done to determine the optimal design choices. Material selection and their justification is presented. Vacuum bagging was identified as the most suitable manufacturing method, considering its cost-effectiveness and ability to produce high-quality laminates. The results from the theoretical calculations, simulations are discussed. Future endeavors include optimizing the layup configuration and conducting simulations to assess the impact of door cutout positions on stress concentrations.

## 1. INTRODUCTION

NASA's ACEE (NASA Aircraft Energy Efficiency) Program aimed to build and design composite components for commercial aircraft. Initial parts included fairing panels, spoilers, and skins. The Airbus A310 featured multiple composite parts, followed by the A320 which had an all-composite empennage. Composite materials improved performance in rotorcraft and general aviation. Boeing and Bell used composites in the V-22 airframe, reducing weight, costs, and part count. [46]. Recent advancements in aircraft materials and manufacturing have led to the development of innovative composites, such as Al-based, Mg-based, Ti-based alloys, ceramics, and polymers. These materials have exceptional properties and are widely used in the aerospace industry for cost reduction, weight reduction, and extended component service life. Composites are also used in military and commercial aircraft, as well as Unmanned Aerial Vehicles (UAVs). [47] Aircraft development in the early 1900s used sitka spruce and tightly woven wool fabric with varnish. Aluminum was experimented for weight savings due to limited power [**Starke and Staley**]. Strength-to-weight ratio was the primary criterion. While lightweight is important, current design considers time duration, fuel savings, range, and a history of multiple aircraft accidents. Now, new materials like high-strength aluminum alloys, titanium alloys, and carbon fiber-reinforced polymer composites have significantly enhanced performance. Material properties, chemistry, processing, and component design have led to substantial improvements. Different components have varying loading profiles, necessitating distinct design and materials selection. [48]

The advancements in material selection correspondingly warranted changes and advancements in manufacturing techniques, especially as composites were increasingly inculcated into the design of aircraft. The ATCAS program was sponsored by NASA with a focus on developing cost and weight-efficient composite technologies. Key manufacturing processes included Automated Fiber Placement (AFP) and Resin Transfer Molding for manufacturing of the frames and pultrusion for floor beams. Significant resources were invested into the program to optimize the manufacturing

process to develop and optimize the processes for efficient and reliable fabrication of the composite structures. New manufacturing methods such as Outer-mold-line (OML) and inner-mold-line tooling (IML) were introduced to facilitate sandwich and stiffened-skin structures. The ATCAS program emphasized the importance of balancing and including the discussions of manufacturing considerations and techniques at the design stage itself to improve costing and throughput. [49]

In the following report, the design and analysis of a completely composite-based fuselage section is discussed. Theoretical and Analytical calculations are undertaken to ensure sound understanding and correlation between each other. Further, prospective materials (from the glass fiber family and relevant resin transfer system), fiber orientation, layups, manufacturing techniques and their effects on the strength of the composite are discussed. Analytical simulations and their agreement with theory is also shown. Finally, the manufacturing possibilities and methods are presented for the composite fuselage assembly. Both best cases as well as cost-effective manufacturing methods are shown.

## 2. METHODOLOGY

Design methodology usually started with gaining information on the market's sentiments, and requirements. It is always recommended to gain an insight from the stakeholder's point of view, as the new product generally caters to their requirements. Therefore, the stakeholder sentiments are obtained through a survey known as the Voice of the Customer (VOC), which aims to capture the most critical requirements the stakeholder thinks are an absolute necessity or the bare minimum in any new product introduced to the market. Next, theoretical calculation is undertaken based on metrics which are derived directly from the stakeholder's feedback. This helps in the ideation of an initial iteration for the overall design, providing us with a complete baseline expectation of an agreeable design. Next, 3D simulations are done utilizing commercial software to get an understanding of how the product reacts to various loading conditions. Manufacturing methods are then discussed, in an ideal scenario as well as in the context of what is available at the Composites Manufacturing Laboratory at the University of Illinois.

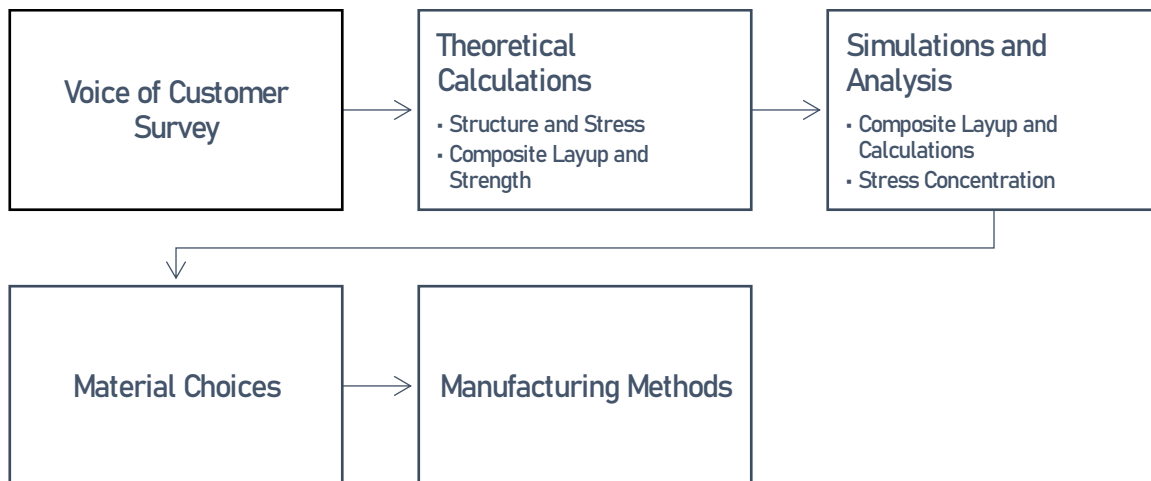


*Figure 1: Methodology of the Fuselage Design Process*

Figure 1 illustrates the overall design process which was followed for the development of the Fuselage.

### 3. IDENTIFYING REQUIREMENTS

There was very little need for a VOC survey in this context, as this design was being developed to be completely in compliance with rules and regulations laid out in the SAMPE Fuselage Design Competition guidelines.

As a result, the basic guidelines and broad constraints for the design were given as the following:

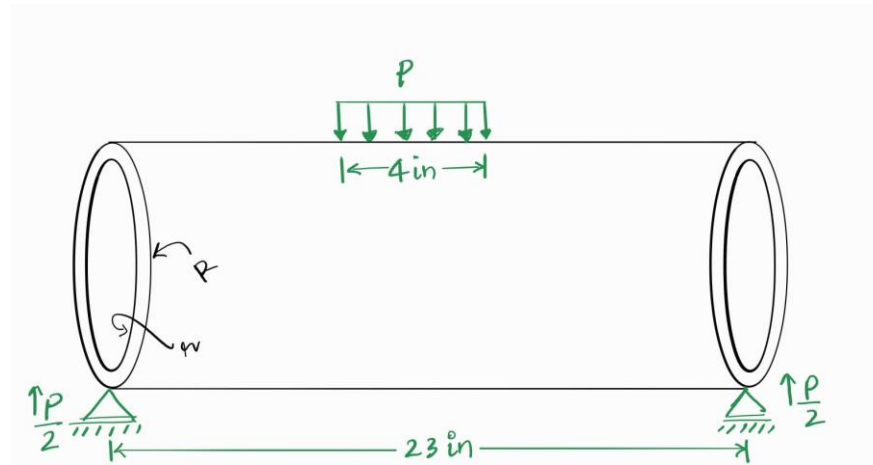
1. The design shall be capable of withstanding at least 1,000 lbf of load.
2. The design shall not deflect more than 1 inch in analysis at load requirement.
3. Fuselage shall be at least 24 inches in length.
4. Inner diameter shall not be less than 5.5 inches throughout the entire length of the fuselage.
5. Outer Diameter shall not be more than 6 inches throughout the entire length of the fuselage.
6. Fuselage shall include 4 cutouts at least 2 inches in diameter each.
7. Cutouts shall be at least 10 inches apart, and no more than 15 inches from each other's closest edges.
8. Cutouts shall be at least 5 inches from the edge of the fuselage.
9. The fuselage shall be made of fiberglass.
10. A Nomex or Kevlar honeycomb core may be used.

The fuselage would be designed considering these initial design parameters.

## 4. CALCULATIONS

### 4.1 Theoretical Calculations

From the above provided requirements, we have a few values to utilize for our theoretical calculations. Consider the figure shown below:



Indenter Load,  $P = 1000 \text{ lbf}$  or  $4448.22 \text{ N}$

Deflection,  $\delta = 1 \text{ in}$  or  $25.41 \text{ mm}$

Length between the two supports of the Bending Fixture,  $L = 23 \text{ in}$  or  $584.2 \text{ mm}$

Inner Diameter,  $r = 5.5 \text{ in}$  or  $139.7 \text{ mm}$

Outer Diameter,  $R = 6 \text{ in}$  or  $152.4 \text{ mm}$

Length of the Fuselage =  $24 \text{ in}$  or  $609.6 \text{ mm}$

The midpoint of the Fixture =  $\frac{L}{2} = 11.5 \text{ in}$  or  $292.1 \text{ mm}$

Following are the assumptions considered:

1. The material is Isotropic.
2. There are no laminates here, and the calculation done is for a solid hollow cylinder.
3. The distributed load while calculating has been normalized into a point load at the center of the fuselage.

*Force measurement in the Y direction (The Reaction force direction of  $\frac{P}{2}$ ) is given by:*

$$P - R_A - R_B = 0$$

$$\text{or } P - \frac{P}{2} - \frac{P}{2} = 0$$

$$\text{or } 4448.22 = P.$$

$\therefore$  the equation is balanced.

The Moment for B is given by:

$$4448.22 \times 292.1 - \frac{P}{2} = 649662.531 \text{ Nmm}$$

The neutral axis,  $y = 152.4 \text{ mm}$

$$I = \frac{\pi}{4} \times [(76.2)^4 - (69.85)^4] = 7783205.4141 \text{ mm}^4$$

$$\therefore \sigma = \frac{M \times y}{I}$$

$$\text{or } \sigma = \frac{(649662.531 \times 76.2)}{7783205.4141} = 6.3604 \text{ MPa}$$

$$\text{We know that } \delta = \frac{FL^3}{48EI}$$

$$\text{or } E = \frac{FL^3}{48 \times \delta \times I}$$

$$\text{or } E = \frac{4448.22 \times (584.2)^3}{48 \times 25.4 \times 7783205.4141}$$

$$\text{or } E = 93.4625 \text{ MPa}$$

This initial calculation of the fuselage assumes a case of pure bending, typical for isotropic materials, e.g., steel. However, since the fuselage is going to be made of multiple layups of composite material, there will be out-of-plane forces involved making it imperative to consider the shear forces involved in future analyses.

Therefore, it is desirable that the effective Young's modulus must incorporate not only the shear modulus but also the geometric factors (there are going to be cutouts in the final product) more accurately to reflect the behavior of the fuselage composite. Composites inherently show anisotropic properties, meaning stiffness and strength varying in direction. For the composite calculations executed, the team also felt that it was necessary to incorporate a factor of safety to account for some terms which were not considered. This also accounts for any other issues which may be encountered such as manufacturing defects, voids, and other environmental influences. The factor of safety also increases the fuselage's ability to withstand loads.

Moreover, the requirement for cutouts introduces localized stress concentration around the perimeter of the cutout, which can be characterized by the stress concentration factor  $k_t$ , which

for circular geometries is approximately 3. This elevated stress must be factored into the bending stress to compute an effective bending stress especially when evaluating first ply failure.

## 4.2 Composite Analysis

The team followed reference [44] for the calculation of the composite layup. The paper was able to adapt the CLT usually used for a flat plate to the shape of a hollow cylinder among other shapes. The paper has experimental results to prove that the deflection was consistent with the analytical results up to a certain limit. The equation given by the paper for a Composite Tube for identifying the maximum deflection was:

$$w_t = P \left\{ \frac{R_m}{16\lambda E_y W_a T} \left[ (3\pi - 8) \left( \frac{R_m}{e} + 1 \right) + \left( \frac{k\pi E_y}{G_{yz}} \right) \right] + \left[ \frac{L^3}{48(EI)_{eq}} + \frac{L}{4(GA)_{eq}} \right] \right\}$$

$$\text{where } e = R_m - \frac{T}{\ln \frac{R_m + 0.5T}{R_m - 0.5T}}, \lambda = 6.74 \left( \frac{R_c}{R_m} \right) + 1.01$$

$$(EI)_{eq} = \pi \left( A_{11} - \left( \frac{A_{12}^2}{A_{22}} \right) \right) R_m^3 + 2\pi \left( B_{11} - \frac{B_{12}^2}{B_{22}} \right) + \frac{\pi}{R_m} \left( D_{66} - \frac{(D_{26})^2}{D_{22}} \right)$$

$$+ \pi \left( A_{55} - \left( \frac{A_{45}^2}{A_{44}} \right) \right) R_m$$

$$E_y = \frac{1}{a_{22}^* T}, G_{yz} = \frac{1}{a_{44}^* T}$$

The best composite layup would be the layup producing the least deflection of all. Therefore, the team created an iterative program in Python which iterated through all possible stack orientations, calculating the deflection for each iteration. Since there was also a core to be used in the layup, most of the available thickness was taken up by the core, allowing only for 4 plies to be used on each half of the composite fuselage.

Due to the inability of some composite packages available on python to consider a core material as part of the entire composite, two separate variations of the code were tried to solve the same problem of including the core as part of the ABD matrix. Silva et. al [45] devised a method in which they added the two ABD matrices of the core and the composite ply layup separately, along with a residual term added to adjust the entire equation. Instead of calculating the residual term as given, the team decided it was best to consider a factor of safety while calculating the equivalent Young's modulus, as not including the term simply underestimated the modulus value.

The code based on the Composipy package and the equations from Zhu's paper yielded differing results based on the material properties entered. It was observed that we cannot escape the issue of the core being considered as one of the plies in the composite. This is an issue as the core does not contribute much to the integral properties of the composite itself, contributing to reducing the shear loading and the load distribution of the composite. Its other inferior properties such as E1 and E2 are very low in comparison to the S-glass/Epoxy properties. The codes can be perused in the Appendix section.

## 5. SIMULATION ANALYSIS

To validate the results and to verify whether the theoretical results agree with real-world, a few simulations were carried out. ABAQUS was used, as it has a simplified interface to model the layup of composites. The simulations showed that the average deformation irrespective of the layups (two layups with the core in between: [0/45/-45/90]s and [0/0/0/0]s ) was in the range of 2.5 mm. The stress increased when the plies were changed to be angled. This could be due to the interlaminar shear stresses between each ply, which could increase due to the orientation.

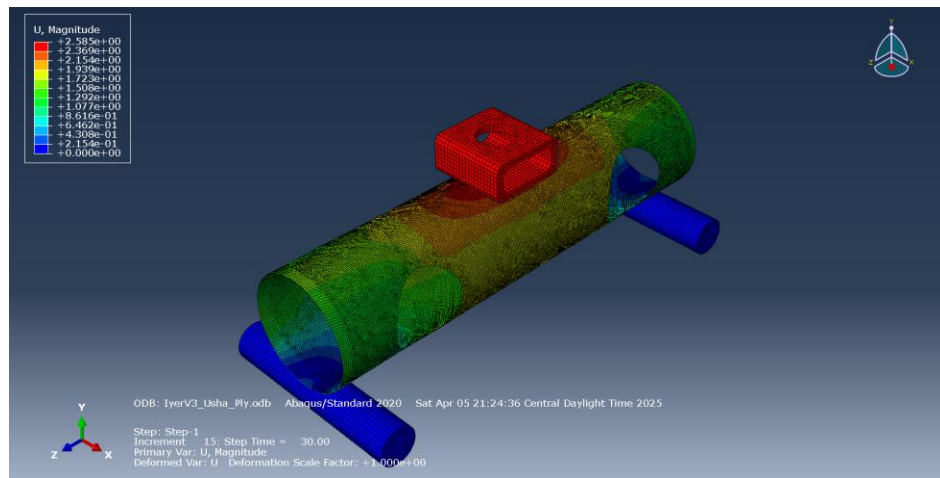


Figure 2: Maximum Displacement for the Ply Orientation [-45/0/45/90/Core/90/45/0/-45]

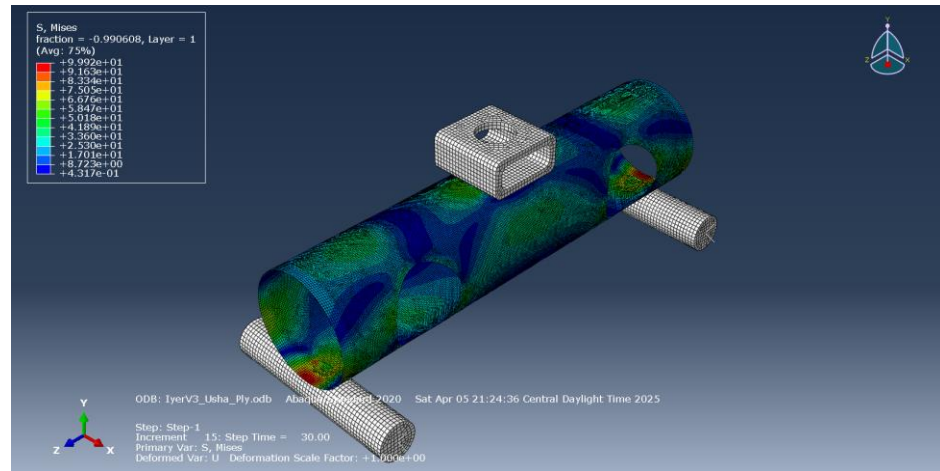


Figure 3: Stress Distribution for the Ply Orientation [-45/0/45/90/Core/90/45/0/-45]

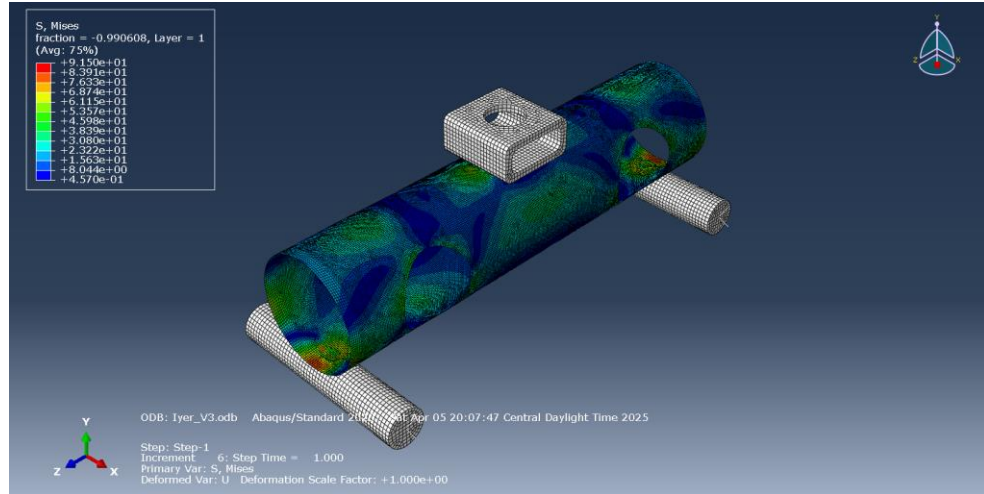


Figure 4: Stress Distribution for the Ply Orientation [0/0/0/0/Core/0/0/0/0]

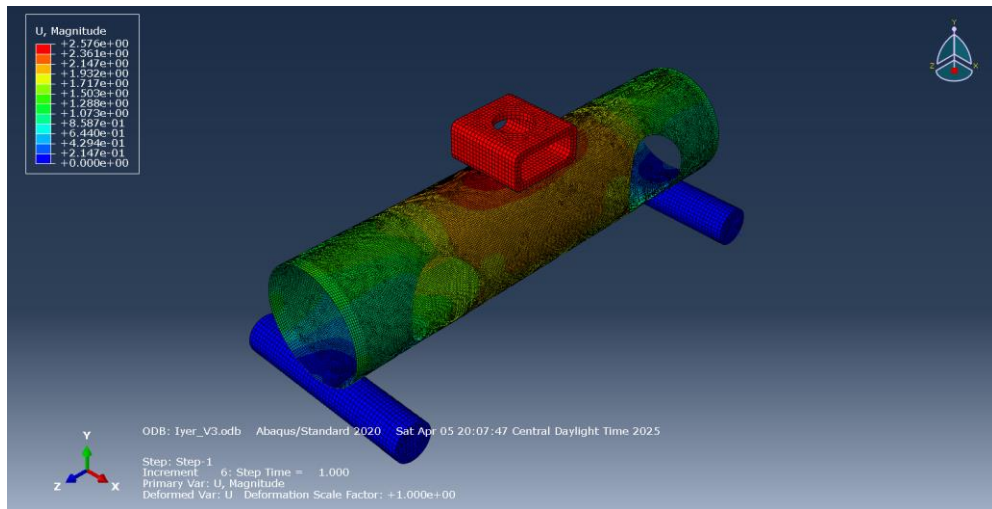


Figure 5: Maximum Displacement for the Ply Orientation [0/0/0/0/Core/0/0/0/0]

More research revealed that the core should have been modelled directly into the laminate assembly and therefore could have provided more accurate results. This should have been included previously, however due to a lack of time, it was not executed. Future work for the Manufacturing Report could include a simulation with respect to the same.

## 6. FIRST PLY FAILURE

A Glass fiber reinforced Epoxy laminate composed of 8 layers, including a core layer, was analyzed to determine the first ply to fail under bending loads by Tsai-Wu failure criterion. Each layer was defined by material properties in the local fiber axes and by an orientation angle measured relative to the global x-y axes. The procedure involved assembling the laminate stiffness matrices, computing curvatures from the applied bending moments, finding the global and then local stresses in each ply, and finally applying a failure criterion to identify the first layer that exceeds its allowable stress limits.

The analysis was implemented in Python using NumPy for matrix computations. The full stacking sequence, stiffness matrix assembly, curvature computation, and Tsai-Wu failure evaluation were automated. Stress and strain results were calculated for each ply under pure bending. Code can be found in the Appendix.

The compliance matrix  $S$  for each layer in local coordinates was constructed as follows. A unidirectional ply exhibits orthotropic behavior in its plane. Let  $E_1$ ,  $E_2$ ,  $G_{12}$ , and  $\nu_{12}$  be its In-plane moduli and Poisson ratio, respectively. Then the local compliance matrix is

$$S_{11} = \frac{1}{E_1} \quad S_{22} = \frac{1}{E_2} \quad S_{12} = \frac{-\nu_{12}}{E_1} \quad S_{66} = \frac{1}{G_{12}}$$

The inverse of  $S$  was computed to give the local stiffness matrix  $Q$ .

$$[Q] = [S]_{\text{plane stress}}^{-1}$$

A unidirectional layer oriented at an angle  $\theta$  in the global x-y plane requires a transformation to obtain its global stiffness matrix  $\bar{Q}$ .

$$[\bar{Q}] = [T]^{-1}[Q][T^*]$$

$$[T]^{-1} = \begin{bmatrix} m^2 & n^2 & -2mn \\ n^2 & m^2 & 2mn \\ mn & -mn & m^2 - n^2 \end{bmatrix} \quad [T^*] = \begin{bmatrix} m^2 & n^2 & mn \\ n^2 & m^2 & -mn \\ -2mn & 2mn & m^2 - n^2 \end{bmatrix}$$

$$m = \cos \theta \quad n = \sin \theta$$

The laminate stiffness matrices A, B, and D were obtained by numerical integration through the thickness. Suppose the z coordinate is defined with the mid-plane at  $z = 0$ . For each layer k with a bottom surface  $h_{k-1}$  and a top surface  $h_k$ , the stiffness integrals were carried out:

$$A_{ij} = \sum_{k=1}^n \bar{Q}_{ij}^k (h_k - h_{k-1})$$

$$B_{ij} = \frac{1}{2} \sum_{k=1}^n \bar{Q}_{ij}^k (h_k^2 - h_{k-1}^2)$$

$$D_{ij} = \frac{1}{3} \sum_{k=1}^n \bar{Q}_{ij}^k (h_k^3 - h_{k-1}^3)$$

The sum of thicknesses from the bottom layer to the top produces the total laminate thickness, and the mid-plane defines  $z = 0$ .

In this case, one of the layers was designated as the core. Its thickness was larger than the surrounding plies, but its in-plane moduli were relatively small. This difference was reflected in its lower  $\bar{Q}$  contribution to A, B, and D. The resulting overall stiffness matrices included the entire stack, from bottom lamina through the core to the top lamina.

$$\begin{Bmatrix} N_x \\ N_y \\ N_{xy} \\ M_x \\ M_y \\ M_{xy} \end{Bmatrix} = \begin{Bmatrix} A_{11} & A_{12} & A_{16} & B_{11} & B_{12} & B_{16} \\ A_{12} & A_{22} & A_{26} & B_{12} & B_{22} & B_{26} \\ A_{16} & A_{26} & A_{66} & B_{16} & B_{26} & B_{66} \\ B_{11} & B_{12} & B_{16} & D_{11} & D_{12} & D_{16} \\ B_{12} & B_{22} & B_{26} & D_{12} & D_{22} & D_{26} \\ B_{16} & B_{26} & B_{66} & D_{16} & D_{26} & D_{66} \end{Bmatrix} \begin{Bmatrix} \varepsilon_x^o \\ \varepsilon_y^o \\ \gamma_{xy}^o \\ \kappa_x \\ \kappa_y \\ \kappa_{xy} \end{Bmatrix}$$

Being a symmetric laminate, the B vector was equal to zero. With A, B, and D known, a pure bending case with no in-plane loads was considered. The bending moment vector M was applied as per the loading conditions specified in the theoretical calculations.

The laminate curvature vector was solved from

$$\begin{Bmatrix} M_x \\ M_y \\ M_{xy} \end{Bmatrix} = \begin{bmatrix} B_{11} & B_{12} & B_{16} \\ B_{12} & B_{22} & B_{26} \\ B_{16} & B_{26} & B_{66} \end{bmatrix} \begin{Bmatrix} \varepsilon_x^o \\ \varepsilon_y^o \\ \gamma_{xy}^o \end{Bmatrix} + \begin{bmatrix} D_{11} & D_{12} & D_{16} \\ D_{12} & D_{22} & D_{26} \\ D_{16} & D_{26} & D_{66} \end{bmatrix} \begin{Bmatrix} \kappa_x \\ \kappa_y \\ \kappa_{xy} \end{Bmatrix}$$

In-plane strains at a distance  $z$  from the mid-plane were then calculated. For each ply, including the core, its local stiffness  $\bar{Q}$  was applied to this global strain to compute the in-plane global stress for each ply are calculated components in  $x$  and  $y$  directions plus  $xy$  shear.

$$\begin{Bmatrix} \varepsilon_x \\ \varepsilon_y \\ \gamma_{xy} \end{Bmatrix} = \begin{Bmatrix} \varepsilon_{0x} \\ \varepsilon_{0y} \\ \gamma_{0xy} \end{Bmatrix} + z \cdot \begin{Bmatrix} \kappa_x \\ \kappa_y \\ \kappa_{xy} \end{Bmatrix}$$

$$\begin{Bmatrix} \sigma_x \\ \sigma_y \\ \sigma_{xy} \end{Bmatrix}_k = \begin{bmatrix} \bar{Q}_{11} & \bar{Q}_{12} & \bar{Q}_{16} \\ \bar{Q}_{12} & \bar{Q}_{22} & \bar{Q}_{26} \\ \bar{Q}_{16} & \bar{Q}_{26} & \bar{Q}_{66} \end{bmatrix}_k \begin{Bmatrix} \varepsilon_x^o \\ \varepsilon_y^o \\ \gamma_{xy}^o \end{Bmatrix} + z \begin{bmatrix} \bar{Q}_{11} & \bar{Q}_{12} & \bar{Q}_{16} \\ \bar{Q}_{12} & \bar{Q}_{22} & \bar{Q}_{26} \\ \bar{Q}_{16} & \bar{Q}_{26} & \bar{Q}_{66} \end{bmatrix}_k \begin{Bmatrix} \kappa_x \\ \kappa_y \\ \kappa_{xy} \end{Bmatrix}$$

A final transformation was then used to convert the global stresses to local fiber axes, that is  $\sigma_1$ ,  $\sigma_2$ , and  $\tau_{12}$ .

$$\begin{Bmatrix} \sigma_1 \\ \sigma_2 \\ \sigma_6 \end{Bmatrix}_k = [T]_k \begin{Bmatrix} \sigma_x \\ \sigma_y \\ \sigma_{xy} \end{Bmatrix}_k \quad [T]_k = \begin{bmatrix} m^2 & n^2 & 2mn \\ n^2 & m^2 & -2mn \\ -mn & mn & m^2 - n^2 \end{bmatrix}_k$$

$$m = \cos \theta_k \quad n = \sin \theta_k$$

A ply failure criterion was applied to the local stress. The Tsai-Wu criterion, which can be stated in polynomial form as

$$f_1\sigma_1 + f_2\sigma_2 + f_{11}\sigma_1^2 + f_{22}\sigma_2^2 + f_{66}\sigma_6^2 + 2f_{12}\sigma_1\sigma_2 = 1$$

Where,

$$\begin{aligned}
 f_1 &= \frac{1}{F_{1t}} - \frac{1}{F_{1c}} & f_{11} &= \frac{1}{F_{1t} F_{1c}} \\
 f_2 &= \frac{1}{F_{2t}} - \frac{1}{F_{2c}} & f_{22} &= \frac{1}{F_{2t} F_{2c}} \\
 f_{66} &= \frac{1}{F_{6u}^2} \\
 f_{12} &\approx -\frac{1}{2} \sqrt{f_{11} f_{22}} = -\frac{1}{2\sqrt{F_{1t} F_{1c} F_{2t} F_{2c}}}
 \end{aligned}$$

The strengths  $F_{1t}$ ,  $F_{1c}$ ,  $F_{2t}$ ,  $F_{2c}$ , and  $F_6$  refer to tensile and compressive strengths in the fiber and transverse directions, plus in-plane shear strength. When the criterion was used, the index for each ply was computed in turn, starting from the bottom to the top. The first ply whose index exceeded 1 was designated as the first ply to fail. If the analysis included a core strength definition, that layer was also checked for in-plane failure; otherwise, the core was treated as having negligible in-plane strength and excluded from the failure checks.

This methodology accounted for each layer's orientation, thickness, and stiffness, along with in-plane strengths in the fiber directions and shear. By computing local stresses under bending and testing them against these allowable limits, the analysis indicated which ply or layer including the core reached its critical stress level first.

A Classical Laminate Theory-based analysis was conducted to evaluate first ply failure under pure bending for various ply orientations. Multiple stacking sequences were examined, incorporating both symmetric and asymmetric configurations. Among the tested layups, the symmetric configuration  $[0^\circ/45^\circ/90^\circ/45^\circ]_s$ , including a core layer, was found to be structurally effective under the applied maximum bending load. The stress distribution across the laminate thickness was assessed using the Tsai-Wu failure criterion, and no plies were found to fail at the specified loading conditions. Additionally, the computed maximum mid-plane deflection under this loading was 23 mm, indicating sufficient stiffness while maintaining failure resistance. This configuration can therefore be considered suitable for applications requiring both mechanical performance and reliability under flexural loads.

## 7. MATERIAL CONSIDERATION

### 7.1 Fiber Selection for Composite Fuselage

In composite structures, the choice of fiber reinforcement plays a critical role in determining mechanical performance, cost efficiency, and manufacturability. While high-performance fibers such as carbon fiber offer exceptional strength-to-weight and stiffness-to-weight ratios, their high cost often makes them impractical for certain applications. In this project, material selection was guided by established design guidelines, which specified fiberglass as the preferred reinforcement category. Among the available options, glass fibers were selected for further study as the primary reinforcement material due to their favorable balance of mechanical properties, cost-effectiveness, and availability. This makes them particularly well-suited for aerospace applications such as fuselage fabrication, where reliable performance must be achieved within budget and production constraints.

Glass fibers are recognized for their high tensile strength, good impact resistance, and ease of processing. Moreover, their widespread availability ensures a cost advantage over advanced fibers such as carbon or aramid. Among the glass fiber variants employed in aerospace applications, S-Glass and E-Glass are most frequently chosen due to their mechanical performance, cost-effectiveness, and widespread availability. These fibers fulfill demanding requirements for structural components, including high tensile strength, stiffness, and impact resistance.

#### **Comparison of S-Glass vs. E-Glass:**

Because of their extensive use and relevance to aerospace engineering, comparing S-Glass and E-Glass is crucial for identifying which fiber best satisfies the performance and cost targets of the fuselage design. This assessment focuses on key parameters such as tensile strength, stiffness, density, and impact resistance.

Mechanical Properties: Comparison of Key metrics from literature review :

Property	S-Glass	E-Glass	Advantage
Tensile Strength	4600 Mpa	3400 Mpa	+35% stronger
Elastic Modulus	89 Gpa	72 Gpa	+23% stiffer
Density	2.53 g/cm <sup>3</sup>	2.54 g/cm <sup>3</sup>	Almost same
Impact Resistance	High	Moderate	Better Durability

*Table 1: Comparison of mechanical properties of S-glass and E-glass*

**Design-Specific Advantage:**

S-Glass offers several distinct benefits over E-Glass for aerospace applications. Its 5.2% elongation, compared to E-Glass's 4.7%, improves impact resistance in multidirectional laminates, while its higher fiber toughness reduces the risk of delamination during manufacturing. Additionally, its 30% greater compressive strength contributes to enhanced structural integrity around door openings and other high-stress areas.

After comparing S-Glass and E-Glass, S-Glass was chosen as the primary fiber for the fuselage design because of its superior mechanical properties. Its 35% higher tensile strength delivers a greater load-bearing capacity under bending forces, and the 23% increase in elastic modulus improves bending resistance while reducing deflection. Furthermore, its enhanced impact resistance makes S-Glass well-suited for regions experiencing stress concentrations or sudden loads, such as door cutouts or structural joints. Building on this selection, the next step involved evaluating different S-Glass variants to determine the most suitable option for the project.

**Comparison of S-Glass Variants:**

S-glass identified as the primary reinforcement material; the next step involves selecting a specific variant that best aligns with the fuselage design requirements. Different S-glass variants offer distinct properties optimized for various composite applications, where factors such as weave type, tensile strength, drapability, and cost can significantly affect the overall laminate performance. Comparing these variants enables the optimization of material selection by balancing design objectives and manufacturing processes. This below table examines three prominent S-Glass variants—AGY S-2 Glass, Hitex HS4 (SW220C), and Hexcel HexForce to determine which most effectively meets performance and manufacturing demands.

S-Glass Variants comparison table:

Variant	Tensile strength	Elastic Modulus	Density	Key Features	Relevance to our Project
AGY S-2 Glass	4890 MPa	89 GPa	2.49 g/cm <sup>3</sup>	Aerospace grade and High fatigue resistance	Best for load compliance Highest strength/stiffness. Reduces laminate thickness for outer diameter compliance.
Hitex HS4 (SW220C-90a)	4200 MPa	88 GPa	2.53 g/cm <sup>3</sup>	4HS weave for drapability. Optimized for impact resistance.	Balanced choice. Stronger than E-Glass, easier to handle and cost-effective.
Hexcel HexForce S-Glass	3500-4000 MPa	85 Gpa	2.63 g/cm <sup>3</sup>	Plain weave. Options for pre-preg. Lower cost	Moderate Performance gains over E-glass and meets all project requirements.

Table 2: Comparison of properties of S-glass variants.

Based on the preceding comparison, AGY S-2 glass was selected for the fuselage design because of its superior mechanical properties. Its tensile strength of 4890 MPa, combined with an elastic modulus of 89 GPa, achieves an optimal stiffness-to-weight ratio. The lower density (2.49 g/cm<sup>3</sup>) further helps reduce overall laminate weight while maintaining structural integrity. In addition, its aerospace-grade quality and fatigue resistance make it particularly suitable for critical load-bearing sections, such as fuselage skins around door cutouts. Although other variants such as Hitex HS4 may offer advantages in drapability or cost, AGY S-2 Glass delivers the high-performance characteristics necessary to minimize laminate thickness while maximizing stiffness and strength.

## 7.2 Core Material:

Core materials play a crucial role in sandwich composite structures, providing a lightweight means of achieving the required strength, stiffness, and energy absorption. When developing high-performance sandwich structures, engineers commonly use materials like aluminum honeycomb

cores due to their strength-to-weight ratio and cost-effectiveness. Polymer foam cores such as polymethacrylimide (PMI) foams are also frequently chosen for applications requiring superior mechanical properties, however the current guidelines constraints limit the choice to Nomex and Kevlar honeycomb cores. Hence are studied further to optimize the fuselage structure effectively.

Nomex and Kevlar honeycomb cores are frequently utilized in aerospace applications due to their favorable strength-to-weight ratios, fire resistance, and durability. Each variant presents distinct advantages and limitations, making a detailed comparison essential to identify the most suitable material for specific fuselage sections.

Property	Nomex Honeycomb core	Kevlar Honeycomb core
Shear Strength	1.25 MPa (L-direction), 0.73 MPa (W-direction)	1.75 Mpa (L-direction) (40% higher) . 1.02 MPa (W-direction)
Compressive Strength	2.4 MPa	3.36 MPa (40% higher than Nomex)
Density	48 kg/m <sup>3</sup> (Commercial grade)	29-128 kg/m <sup>3</sup> (Customizable based on size and thickness)
Cost	Lower (63.50 per sheet for 5mm thick and 48 kg/m <sup>3</sup> )	20-30% higher than Nomex
Thermal Resistance	Service temperature: up to 180°C	Comparable to Nomex with better thermal stability under continuous exposure
Flame Resistance	Self-extinguishing to FAR 25.583 standards	Comparable to Nomex®, meets aerospace fire safety standards
Corrosion Resistance	Good moisture resistance with proper sealing	Excellent, resistant to chemical corrosion and environmental degradation.
Electrical Insulation	Moderate	High, suitable for electromagnetic shielding applications

Machining Difficulty	Moderate; easier to machine due to moderate rigidity	High; requires specialized tools due to abrasive nature and fragile cell walls.
----------------------	--	---

*Table 3: Comparison of properties of Kevlar and Nomex Honeycomb cores.*

Based on the comparative analysis above, Nomex honeycomb cores are well suited for cost-sensitive applications demanding moderate strength and stiffness, making them ideal for fuselage components such as cabin floors and bulkheads. Kevlar honeycomb cores, in contrast, are more appropriate for high-stress regions requiring maximum shear strength and superior compressive performance. Strategic allocation of these materials ensures optimized structural efficiency and performance while complying with relevant design and material constraints

### 7.3 Introduction to Resin selection

Resins play a critical role in composite structures by binding reinforcing fibers, transferring loads between fibers, and providing protection against environmental factors. The resin matrix significantly influences the overall mechanical properties, chemical resistance, and thermal stability of composite materials. In aerospace applications, where high strength-to-weight ratios and durability are paramount, selecting an appropriate resin system is essential for maintaining structural integrity and optimal performance.

The resin systems selected for comparative analysis below were chosen based on their relevance to aerospace applications and their capability to satisfy specific performance criteria for composite fuselage structures. Epoxy, vinyl ester, polyester, and polyurethane resins were compared based on their mechanical properties, chemical resistance, and compatibility with S-glass fibers. By comparing these resin systems in terms of tensile strength, elastic modulus, shrinkage, chemical resistance and manufacturability, the analysis aims to determine the most suitable resin for fuselage design applications.

## Rationale table for different types of resin systems:

Resin	Tensile Strength (MPa)	Elastic modulus (GPa)	Shrinkage	Chemical resistance	Compatibility with Fiber (S-Glass)	Performance Summary
Epoxy	70-100	3-4	<1%	Excellent resistance to moisture, solvents, and high temperatures (up to 150°C)	Fully compatible with S-glass; forms strong bonds with fibers due to high adhesion properties. Quick wet-out ensures uniform fiber impregnation	High strength and stiffness and strong bonding with S-glass minimizes delamination risks.
Vinyl Ester	60-80	2.5-3	<2%	Excellent resistance to acids, alkalis, and solvents	Fully compatible with S-glass; provides good fiber wet-out and adhesion	Affordable and tough but lower stiffness may result in higher deflection under load.
Polyester	40-70	2-2.5	~4%	Poor to moderate chemical resistance; susceptible to degradation over time in harsh environments	Limited compatibility with S-glass; weaker bonding compared to epoxy or vinyl ester	Limited mechanical performance
Polyurethane	~50	~1.5	<1%	Good resistance to solvents but limited durability	Compatible but does not provide strong bonding strength compared to epoxy or vinyl ester	Tough but lacks stiffness required for structural applications.

				under loads	cyclic		
--	--	--	--	----------------	--------	--	--

*Table 4: Comparison of properties of different resins*

Based on the comparative analysis presented, epoxy resin demonstrates the highest mechanical performance among the evaluated options, aligning well with the requirements for composite fuselage designs. Its enhanced tensile strength and elastic modulus as detailed in above table ensure the stiffness and strength essential for load-bearing fuselage structures. Additionally, epoxy resin provides superior bonding capabilities with S-glass fibers effectively, minimizing the risk of delamination. Its compatibility with vacuum bagging techniques further contributes to a reliable and consistent manufacturing process. Although other resin systems possess certain advantages such as the cost effectiveness of polyester or the toughness characteristics of polyurethane, epoxy resin offers the most balanced and advantageous set of properties, meeting the demanding performance criteria required for aerospace fuselage applications.

#### 7.4 Composite Layup Design:

Designing an effective composite layup for the fuselage is crucial for achieving the required structural performance while minimizing weight. This section presents the rationale behind the chosen layup design, examines the role of individual ply orientations and describes the methodology for optimizing the stacking sequence.

**Role of Ply orientation in composite laminates:**

Composite laminates derive their unique mechanical characteristics from the orientation of the individual plies. Each ply orientation addresses a specific structure need, contributing to the overall performance.

**0° Plies:** the primary function of 0° plies is to carry axial loads along the fuselage's longitudinal axis. By aligning fibers at 0°, these plies maximize tensile and compressive strength in that direction, effectively resisting bending forces. However, an overreliance on 0° plies can concentrate stresses at ply interfaces, increasing the likelihood of delamination. Consequently, these plies are typically complemented by other orientations to mitigate stress concentrations.

**45° Plies:** plies oriented at 45° are essential for resisting shear forces and enhancing impact resistance. Shear stresses arise from in-plane loads acting parallel to a surface, and ±45° orientations distribute these forces more effectively. These plies also dissipate energy during impacts and dynamic loading, making them especially important in areas prone to shear forces or sudden loads, such as door cutouts or structural joints.

**90° plies:** Plies oriented at 90° provide lateral stability by resisting transverse loads perpendicular to the primary load direction. Although they contribute minimally to bending stiffness, these plies

help maintain structural stability in cylindrical fuselage designs by counteracting hoop stresses from internal or external forces.

#### Multidirectional Layups:

Combining  $0^\circ$ ,  $\pm 45^\circ$ , and  $90^\circ$  plies in a symmetric, balanced configuration provides an optimal balance of stiffness, strength and weight. A commonly recommended stacking sequence is [0/45/90/45] s, which leverages  $0^\circ$  plies for axial stiffness,  $45^\circ$  plies for shear strength and impact resistance, and  $90^\circ$  plies for lateral stability. This approach minimizes stress concentrations and achieves more uniform load distribution.

Experimental evaluations show that while unidirectional laminates (12) offer high flexural strength, they are prone to brittle failures under transverse loads. Multidirectional laminates on the other hand, distribute stresses across various fiber orientations, thereby improving damage tolerance and reducing the risk of delamination.

#### Layers and thickness Optimization:

The total number of layers in a composite laminate significantly influences bending stiffness and overall mass. A minimum of three plies (approximately 0.53 mm in thickness) is necessary to prevent porosity and moisture ingress, thus preserving structural integrity. For aerospace fuselages exposed to bending and impact loads, 36-40 layers typically provide a suitable balance between stiffness and weight.

#### *Symmetry:*

Symmetric and balanced layups are pivotal for minimizing residual stresses and preventing delamination during manufacturing or under operational loads. Symmetry helps distribute curing and thermal expansion stresses evenly throughout the laminate, reducing the likelihood of warping or twisting.

## 8. MANUFACTURING

### 8.1 Introduction to Manufacturing Plan Selection

This section analyzes potential manufacturing methods for fabricating a high-performance composite fuselage, integrating considerations of structural integrity, cost-effectiveness, design flexibility, and process scalability. Various methods are evaluated based on their alignment with design and performance objectives, and efficiency in resource usage. The final selection is justified through a structured decision matrix that accounts for critical factors identified in the literature review.

The manufacturing methods which were considered for this decision matrix are:  
Change the order and write that which are most suitable in the beginning

1. Vacuum Bagging
2. Additive Manufacturing
3. Automated fiber placement (AFP)
4. Resin Transfer Molding (RTM)
5. Filament Winding
6. Hand Layup

The literature review identified vacuum bagging as the most efficient manufacturing method for composite fuselage structures due to its optimal balance of quality, performance, and cost-effectiveness. Vacuum bagging is good in producing high-strength, lightweight components characterized by uniform thickness and minimal defects, qualities particularly important in aerospace applications. To ensure a good understanding of the available manufacturing methods, this section briefly introduces each method, focusing on their respective processes, advantages, disadvantages, and suitability for fuselage manufacturing. Methods such as hand layup, resin transfer molding (RTM), filament winding, additive manufacturing (3D printing), and automated fiber placement (AFP) are studied to provide a comparative analysis that highlights their relative strengths and limitations within the context of fuselage manufacturing. This comparative overview establishes the rationale for selecting vacuum bagging as the preferred technique while recognizing the specific advantages of alternative manufacturing methods for specialized applications.

## Vacuum Bagging

The vacuum bagging process involves sealing layers of fiber under a vacuum bag to ensure uniform pressure during curing. This technique is designed to consolidate the laminate effectively while simultaneously removing excess resin and trapped air. By creating a controlled environment under vacuum pressure, the fibers are compressed uniformly, resulting in a more compact and cohesive structure. The vacuum bag acts as a barrier, maintaining consistent pressure throughout the curing process, which is critical for achieving optimal laminate quality.

Vacuum bagging offers several advantages over traditional hand layup methods. One of its key benefits is improved consolidation, which leads to reduced void content within the laminate. This results in a stronger and more durable composite structure. Additionally, vacuum bagging provides more consistent thickness across the laminate compared to hand layup techniques, ensuring uniformity in structural properties. The method also delivers higher strength-to-weight ratios and more consistent quality, making it particularly beneficial for medium-sized fuselage structures. However, there are some disadvantages associated with this process. Vacuum bagging requires additional equipment such as vacuum pumps and bagging film, which can increase costs slightly compared to hand layup methods. Furthermore, operator proficiency is essential to prevent leaks during the process, as the maximum pressure achievable is limited to atmospheric pressure (approximately 14.7 psi).

Vacuum bagging is commonly employed for primary fuselage structures where moderate strength and weight efficiency are essential. Its ability to produce consistent and high-quality laminates makes it an ideal choice for applications requiring reliable performance in medium-sized composite components. While it may not be suitable for all manufacturing scenarios due to its equipment requirements and cost considerations, vacuum bagging remains a preferred method for achieving structural integrity in aerospace applications where strength-to-weight ratios are critical.

## Additive Manufacturing (3D Printing):

Additive manufacturing, commonly referred to as 3D printing, is a process in which composite materials, such as carbon fiber-reinforced thermoplastics, are deposited layer by layer to construct parts. This technique eliminates the need for extensive tooling and allows for the precise fabrication of components directly from digital designs. By building parts incrementally, additive manufacturing offers a highly controlled and efficient method for producing composite structures while minimizing material waste.

The advantages of additive manufacturing are significant, particularly in terms of design flexibility. This method enables the creation of intricate geometries and integrated features that would be challenging or impossible to achieve with traditional composite fabrication techniques. Additionally, additive manufacturing excels in rapid prototyping, allowing engineers to quickly test and iterate designs with minimal material waste. Despite these benefits, there are notable disadvantages. The mechanical properties of parts produced through additive manufacturing may

be inferior to those achieved using conventional composite methods. Furthermore, this process is generally restricted to smaller scale parts and offers limited material options compared to traditional techniques.

Additive manufacturing is particularly suited for prototyping fuselage components that require complex internal structures or lightweight core designs. Its ability to produce intricate geometries and lightweight parts makes it ideal for applications where design complexity and efficiency are prioritized. While it may not be suitable for large-scale production or high-performance structural components due to its limitations in mechanical properties and material selection, additive manufacturing remains a valuable tool for innovation in aerospace prototyping and lightweight design.

#### Automated Fiber Placement (AFP):

Automated Fiber Placement (AFP) is a highly advanced manufacturing process that utilizes robotic systems to deposit prepreg tapes onto a mold with exceptional precision. This process involves controlling fiber orientation and thickness to ensure optimal structural performance. The fibers, typically carbon or glass, are pre-impregnated with resin and placed in narrow strips, known as "tows," which are compacted and heated during the deposition process. The robotic system ensures repeatable accuracy, enabling the fabrication of complex geometries and high-quality composite structures. AFP is widely employed in aerospace manufacturing to create large-scale components such as fuselage sections and wing spars, where precise material placement is critical for achieving desired mechanical properties [3][5][7].

AFP offers numerous advantages that make it a preferred method for composite manufacturing in aerospace applications. Its unmatched precision in fiber placement minimizes material waste and ensures consistent quality across large, complex structures. This precision also allows for optimized fiber orientations, enhancing the strength-to-weight ratio of the final product. Additionally, AFP significantly reduces production time compared to manual methods, as robotic systems can operate continuously with minimal downtime [2][5][6]. However, AFP comes with notable disadvantages. The equipment and operational costs are extremely high, requiring substantial capital investment. Furthermore, skilled operators and programming expertise are essential to manage the system effectively and prevent defects such as material wrinkling or gaps during the layup process [4][6][7].

AFP is particularly suitable for manufacturing large composite structures in the aerospace industry, where weight optimization and repeatability are paramount. Its ability to produce high-performance laminates with precise fiber orientations makes it ideal for fuselage sections, wing spars, and other critical components requiring superior mechanical properties. While its high cost

may limit its use outside of industries that can justify such investments, AFP remains an indispensable technology for applications demanding lightweight yet durable structures, such as commercial aircraft and spacecraft.

#### Resin Transfer Molding (RTM):

Resin Transfer Molding (RTM) is a composite manufacturing process that involves positioning dry fibers within a closed mold and injecting resin under pressure to impregnate the reinforcement thoroughly. The resin, often combined with catalysts, flows into the mold cavity to saturate the fiber preform, ensuring uniform distribution and complete impregnation. Once the resin cures, the mold is opened, and the finished component is removed. RTM enables precise control over fiber orientation and resin content, making it suitable for producing high-performance composite parts with excellent dimensional accuracy and surface finishes. This process is widely used in industries such as aerospace, where lightweight and durable components are essential.

RTM offers several advantages that make it a preferred method for composite manufacturing. It produces high-quality parts with consistent dimensions and excellent surface finishes on both sides of the component. The process is particularly well-suited to complex geometries and integrated features, such as door cutouts, due to its ability to mold intricate shapes with tight tolerances. Additionally, RTM minimizes material waste by allowing near-net-shape production, reducing post-processing requirements. However, there are some disadvantages associated with RTM. The initial setup cost is high due to the need for specialized mold fabrication, which can be a barrier for small-scale production or prototyping. Moreover, achieving optimal results requires careful control of processing parameters and skilled operators.

RTM is ideal for manufacturing high-performance fuselage sections that demand tight tolerances and reduced post-processing. Its ability to produce lightweight yet durable components make it particularly valuable in aerospace applications where structural integrity and weight optimization are critical. While its high initial costs may limit its use in certain scenarios, RTM remains indispensable for applications requiring precision-engineered composite parts with complex geometries and superior mechanical properties.

## Filament Winding

Filament winding is a composite manufacturing technique that involves winding continuous fibers, such as carbon, glass, or aramid, onto a rotating mandrel. The fibers are impregnated with resin either before or during the winding process to ensure proper bonding and structural integrity. The mandrel rotates while a carriage system moves horizontally, laying down the fibers in predetermined patterns to achieve the desired orientation and thickness. Once the winding is complete, the resin is cured using heat or other methods, and the mandrel is removed to leave behind a hollow composite structure. This process is particularly effective for creating cylindrical or spherical components with high mechanical strength and precision.

Filament winding offers several advantages, making it an efficient and reliable method for composite manufacturing. It provides high hoop strength due to its ability to optimize fiber placement for cylindrical shapes, making it ideal for pressure vessels or structures subjected to hoop loading. The process efficiently utilizes continuous fibers, resulting in strong and lightweight components with minimal material waste. Additionally, filament winding is highly automated, ensuring repeatable quality and reducing labor costs. However, there are limitations to this method. It is primarily restricted to axisymmetric geometries and cannot accommodate complex shapes with openings, such as fuselage sections with integrated features. Furthermore, filament winding requires specialized equipment, which can be costly to acquire and operate.

Filament winding is particularly suitable for manufacturing fuselage tubes or pressure vessels that demand significant hoop strength and relatively simple geometries. Its ability to produce lightweight yet durable components make it an excellent choice for applications where internal pressure resistance is critical. While its geometric constraints limit its use for more intricate designs, filament winding remains a preferred method for producing high-performance cylindrical structures in industries such as aerospace, automotive, and industrial manufacturing.

## Hand Layup

The hand layup process is one of the simplest and most widely used methods for composite manufacturing. It involves manually placing fiber reinforcements, such as fiberglass or carbon fiber, onto a mold that has been prepared with a release agent to prevent sticking. Resin is then applied using brushes, rollers, or similar tools to impregnate the fibers thoroughly. Additional layers of reinforcement and resin are added sequentially until the desired thickness is achieved. Once the layup is complete, the composite is allowed to cure, either at room temperature or under controlled conditions, before being removed from the mold. This process is straightforward and requires minimal equipment, making it accessible for small-scale production and prototyping.

Hand layup offers several advantages due to its simplicity and low initial cost. It requires minimal equipment and is highly adaptable, allowing for flexibility in layup orientation and design modifications. These characteristics make it particularly suitable for small-scale fuselage sections or prototypes where precision is not critical. However, the process has notable disadvantages. It is labor-intensive and time-consuming, which limits its efficiency for larger-scale production. Additionally, because it relies heavily on manual labor, there is a higher risk of defects such as inconsistent fiber alignment, elevated porosity, and air voids. These issues can result in parts with variable mechanical properties and inconsistent thickness.

The hand layup process is most suitable for producing small fuselage prototypes or non-critical components where tight tolerances and high mechanical performance are not required. Its low cost and adaptability make it an attractive option for experimental designs or projects with limited budgets. However, for applications requiring consistent quality or high production volumes, alternative methods such as vacuum bagging or resin transfer molding may be more appropriate. Despite its limitations, hand layup remains a valuable technique for specific use cases in composite manufacturing due to its versatility and accessibility.

### ***Rationale with decision matrix:***

The selection of the manufacturing method was conducted through a decision matrix which is employed to systematically evaluate each technique against a predefined set of criteria. This structured approach ensures an objective comparison by assigning weights to these criteria based on their relative importance in fuselage manufacturing, including factors such as cost efficiency, Compliance to rules, Quality of Finished Product, and Flexibility in Design. Each manufacturing method is subsequently scored against these weighted criteria to quantify its overall performance. This structured framework facilitates identifying the most effective manufacturing method while offering transparent and justifiable reasoning for the selection process.

Criteria	Weight	Justification
Cost	3	Budget constraints necessitate minimizing material, tooling, and labor costs.
Manufacturing Time	4	Efficient and timely production is a fundamental requirement
Quality of Finished Product	5	As the part needs to withstand load requirement and needs to have minimum defects to produce High quality product
Implementation	4	The method must be feasible given available skills, equipment, and resources.
Flexibility in Design	4	The ability to produce complex geometries (e.g., fuselage cutouts) is advantageous.
Compliance to rules	5	Must comply with established guidelines, requirements, and regulations.

#### Decision Matrix:

The decision matrix below shows the evaluation of various manufacturing methods for fuselage production. Each method is assessed against key performance criteria, with weights assigned to reflect their relative significance in fuselage manufacturing. This comparative framework enables a clear and systematic analysis, supporting the identification of the most appropriate manufacturing technique for fuselage applications.

Method	Cost (4)	Manufacturing Time (4)	Quality (5)	Implementation (4)	Flexibility (4)	Compliance (5)	Total Weighted score
Hand Layup	5	2	2	5	2	5	91
Vacuum Bagging	4	3	4	4	3	5	105
RTM	2	4	4	2	4	4	88
Automated Fiber Placement	1	5	5	1	5	4	93
Filament Winding	3	3	4	3	2	5	89
Additive Manufacturing	2	4	4	3	5	5	101

Table 5: Decision matrix of comparing various manufacturing methods against criteria

Based on the outcomes of the comprehensive decision matrix, vacuum bagging is identified as the most suitable manufacturing method for composite fuselage production. This technique offers an optimal balance of cost efficiency, manufacturing quality, and ease of implementation, aligning well with the rigorous performance requirements of the fuselage. Although additive manufacturing presents significant potential for producing complex geometry and innovative designs, its current limitations in scalability and mechanical performance render it less practical for mid-scale fuselage fabrication. The established reliability of vacuum bagging, along with its capacity to deliver consistent and high-quality results, reinforces its selection as the preferred method for manufacturing high-performance composite fuselages.

## 8.2 Planned processing steps involved in vacuum bagging method:

The following section provides a systematic explanation of each step involved in the manufacturing approach, from material preparation and fiber layup to vacuum sealing and curing. This step-by-step outline illustrates how the method is implemented to optimize structural performance, minimize manufacturing defects, and fulfill the requirements associated with fuselage production.

### *Mold Preparation:*

1. Start by Thoroughly clean the Mold surface with acetone or other solvent
2. Apply Coating or releasing agent at least 2-3 times to avoid sticking and allow each coat to dry completely.
3. Lay Down a layer of mold release film or peel ply which can help in part removal and surface finish.

### *Cutting and Material preparation:*

1. Cut the fiberglass fabric to required dimensions allow extra for trimming
2. Pre-cut peel ply, release film, breather material, and vacuum bagging film

### *Layup:*

1. Apply the first layer of fiberglass fabric on to the mold ensuring no wrinkles.
2. Use a roller to remove any air bubbles.
3. Continue adding layers according to layup configuration [0/90/(±45)2s].
4. Between the layers use a roller to make sure there aren't any air bubbles.
5. Place peel ply over the final layer of fiberglass.

### *Vacuum Bagging setup:*

1. Apply release film over the peel ply.
2. Add breather material over the release film.
3. Position vacuum ports and tubing for even resin distribution.
4. Drape vacuum bagging film over the entire layup
5. Seal edges with sealant tape, making sure it's airtight seal.

*Resin Preparation:*

1. Calculate the required amount of resin based on your layup.
2. According to our manufacturer's specifications mix epoxy resin and hardener.
3. Degas the resin mixture in a vacuum chamber to remove air bubbles.

*Resin Infusion:*

1. Connect the vacuum pump and create an initial vacuum to check for any leaks.
2. Once sealed, inject resin mixture through inlet ports.
3. Monitor the resin flow, make sure it's evenly distributed across the layup.
4. Clamp off resin inlet once resin covers entire layup and wet-out is achieved.

*Curing Process:*

1. Maintain vacuum throughout the curing cycle
2. For heated cure, place the mold in an oven and for room temperature cure allow the part to cure for 24-48 hours.
3. Follow the resin manufacturer's recommended cure cycle for time and temperature of curing.
4. Adjust vacuum pressure as needed or as recommended during cure.

*Post-curing:*

1. Remove the part from the mold after curing
2. Place the part in an oven for any post-curing if it's recommended by the manufacturer.

*Finishing:*

1. Trim excess material using cutting tools.
2. Use sandpaper to smooth the edges for a clean finish.
3. Cut out the door opening according to our calculations.
4. Sand the door openings for a smoother finish.

*Quality control:*

1. Measure the dimensions to ensure they match with our calculations and meet our competition rules.
2. Perform visual inspection for any surface defects.
3. Do the tap testing to check for any voids or delamination.

### 8.3 Identified key risks with impacts

#### *Identification of potential risks in selected manufacturing method:*

Vacuum bagging is a widely used and reliable method for manufacturing composite fuselages. However, certain risks remain inherent to the process. These risks arise from process complexity, environmental factors, and the need for precise execution. Each potential risk is described below, focusing on its relevance to fuselage manufacturing and accompanied by an assessment of its likelihood and impact.

#### *Potential Risks in Vacuum Bagging:*

##### Leaks or Bag failures:

Leaks in the vacuum bag or improper sealing compromise vacuum pressure, leading to insufficient laminate consolidation. Poor compaction can result in voids, reduced mechanical properties, and potential failure under load. Studies indicate that vacuum bag leaks have the greatest negative impact on composite part quality.

Consistent compaction is essential for maintaining uniform strength and stiffness in fuselage sections. However, the likelihood of vacuum bag leaks remains high, primarily due to manual sealing errors or defects in the bag material. When such defects occur, they can have a significant impact, often leading to scrapped parts or a reduction in structural integrity.

##### Uneven Pressure distribution:

Improper placement of breather material or wrinkles in the vacuum bag can create uneven pressure during curing, resulting in localized defects such as resin pooling or dry spots. These flaws weaken the laminate and may form critical failure points.

Uniform pressure distribution is essential for achieving consistent fiber-to-resin ratios across large fuselage components. The likelihood of issues in this area is medium, as outcomes are highly dependent on operator skill and the precision of the setup. The impact, however, is high—any weak spots resulting from inconsistent pressure can lead to delamination or failure under stress.

##### Resin pooling or dry spots:

Incorrect resin application or uneven flow during infusion can cause excess resin (pooling) or insufficient resin (dry spots), reducing laminate stiffness and increasing the risk of delamination. In fuselages, such inconsistencies can compromise reliability under dynamic loads.

The likelihood of issues in this area is medium, as it is influenced by factors such as resin viscosity, flow media design, and operator experience. The impact is also medium, as these issues can reduce the overall strength and durability of the composite structure.

### Surface Finish defects:

Variations in vacuum pressure or curing conditions may produce surface imperfections such as wrinkles or entrapped air. On a fuselage, surface defects could affect both aerodynamic performance and quality, factors that often hold weight in competitions.

A smooth surface finish is important for both aerodynamic efficiency and visual appeal. The likelihood of surface finish issues is low, as they can generally be mitigated through careful setup and ongoing monitoring. The impact is medium—while such imperfections typically have limited structural consequences, they could influence competition scoring.

### Environmental Factors:

Fluctuations in temperature and humidity during curing can affect resin viscosity and curing times, potentially causing incomplete polymerization or inducing thermal stresses in the laminate. Controlled curing environments are critical for maintaining consistent mechanical properties throughout large fuselage structures.

The likelihood of issues arising in this area is medium, as they are heavily influenced by local workshop conditions and the quality of available equipment. The impact is also medium, as inadequate curing may reduce part consistency and affect long-term durability.

**Likelihood and Impact Assessment:** The likelihood and impact of each risk were assessed based on industry data and practical experience:

Risk	Likelihood	Impact	Overall Risk level
Leaks or Bag failure	High	High	Critical
Uneven Pressure distribution	Medium	High	Significant
Resin pooling/Dry spots	Medium	Medium	Moderate
Surface Finish Defects	Low	Medium	Low
Environmental Factors	Medium	Medium	Moderate

*Table 6: Likelihood and Impact Assessment*

## 8.4 Mitigation strategies for the Risks identified:

Mitigation Strategies for Vacuum Bagging Risks:

Leaks or Bag Failures:

Mitigation strategies include the use of automated leak detection systems, such as pressure decay sensors or ultrasonic leak detectors, to identify leaks during setup. Implementing pre-engineered vacuum bag kits with pre-cut materials, such as those offered by Velocity Composites PLC, can help minimize manual errors. Additionally, applying redundant sealing methods—using double-sided adhesive tape and silicone sealant at critical joints—can further reduce the risk of leaks.

Uneven Pressure Distribution:

Mitigation measures include optimizing breather material placement by using flow simulation software to design effective resin flow paths. This helps ensure even distribution and efficient compaction. Additionally, integrating automated pressure monitoring with real-time sensors can help maintain uniform compaction throughout the curing process.

Resin pooling/ Dry Spots:

Mitigation strategies involve simulating resin infusion using tools such as PAM-RTM or ANSYS to predict and prevent the formation of dry spots. Additionally, implementing controlled resin application through metered mixing systems helps maintain consistent resin viscosity and flow rates throughout the process.

Surface Finish defects:

Mitigation involves maintaining controlled curing conditions, with stable temperatures between 20–25°C and humidity levels below 60% during the curing process. Additionally, applying peel ply fabric can help achieve smooth surface finishes.

Environmental Factors:

Mitigation includes using a climate-controlled workspace, supported by portable dehumidifiers and heaters, to stabilize workshop conditions. Additionally, selecting resins with longer pot lives can help accommodate variability in the environment during processing.

## Risk Prioritization Matrix (Likelihood Vs Impact)

The 5x5 Matrix below assesses risks based on their likelihood and Impact, guiding resource allocation for mitigation:

Impact → Likelihood ↓	Very Low (1)	Low (2)	Medium (3)	High (4)	Very High (5)
Almost Certain (5)				Leaking of Vacuum bag/Imperfect Seal	
Likely (4)				Uneven Pressure	
Probable (3)		Environmental factors	Resin Pooling		
Unlikely (2)	Surface Finish Defects				
Very Unlikely (1)					

Table 7: Risk Prioritization Matrix (Likelihood Vs Impact)

The risk assessment matrix for the manufacturing process identifies and categorizes potential issues based on their severity and likelihood of occurrence. The most critical risk is the possibility

of leaks during resin infusion, which could prevent the vacuum bag from holding vacuum and compromise the structural integrity of the part. Significant risks include uneven pressure distribution during curing, which may lead to delamination or inconsistent mechanical properties. Moderate risks such as resin pooling are also noted, as they can cause local increases in weight or reduced fiber volume fraction. Low risks include surface finish imperfections, which primarily affect aesthetics rather than structural performance. Lastly, below moderate risks such as minor environmental factors (e.g., ambient temperature or humidity) are considered less impactful but still monitored to ensure process consistency. This categorization helps prioritize mitigation strategies and informs quality control measures during manufacturing.

## **9. Final Decision on Manufacturing/Literature Review:**

**The team would like to move ahead with Manufacturing.**

## 10. CONCLUSION

A comprehensive design and analysis of a composite Fuselage was presented within the given requirements of the SAMPE design competition. A baseline design derived through requirements was iterated upon thorough theoretical calculations and a thorough literature review. A comprehensive understanding of the behavior and mechanics of the fuselage were obtained through theoretical and simulations. The fuselage structure was engineered using a strategic combination of S-Glass fibers (AGY S-2), Nomex and Kevlar honeycomb cores, and epoxy resin, resulting in a composite that balances rigidity, impact resistance, and cost-effectiveness. The use of a balanced layup sequence  $[0^\circ/45^\circ/90^\circ/45^\circ]$ s further enhanced load transfer efficiency and minimized risks associated with interlaminar failure.

The iterative approach adopted throughout the design process allowed for continual refinement of geometry and material configuration, ultimately yielding a solution that meets both strength and stiffness requirements while minimizing weight.

Simultaneously, Manufacturing considerations were also central to the design process. Vacuum bagging was selected for its ability to produce consistent, high-quality laminates, with specific mitigation strategies implemented to address known manufacturing challenges such as vacuum leakage and pressure inconsistency.

However, the team believes that there are still many avenues for research and further understanding which can be done in the future.

1. Further Optimization study of the Layup of the Composite is required. This is because the optimization carried out in the current report is conservative due to the various assumptions listed in the report during the calculation phase of the design. Further refinement could be done in this area by utilizing better optimization techniques.
2. Further, the simulation done does not consider the different positions of the door cutouts which can be optimized to decrease stress concentration factor.
3. Additionally, the simulation does not consider the cavities present in a honey-comb structure as the core itself is considered a ply in the overall laminate make-up. This is causing an over-prediction of the minimal displacement achieved. Therefore, further study needs to be done in this area by assuming an accurate morphology of the honeycomb structure.
4. Proposed manufacturing methods are based completely on ideal conditions, and on the basis that there was access to the best method available, and the Apparatus and Constraints placed on the team due to the availability of machinery on the campus were not considered for this report. The Manufacturing Report should be more in line with the processes available to us on campus.

**DISCLOSURE: The team would like to disclose that there has been limited and responsible use of Artificial Intelligence agents in the documentation of this project, and as a glorified search engine to identify relevant academic papers efficiently. After obtaining responses, the team carefully verified and vetted all information which has been presented in this report.**

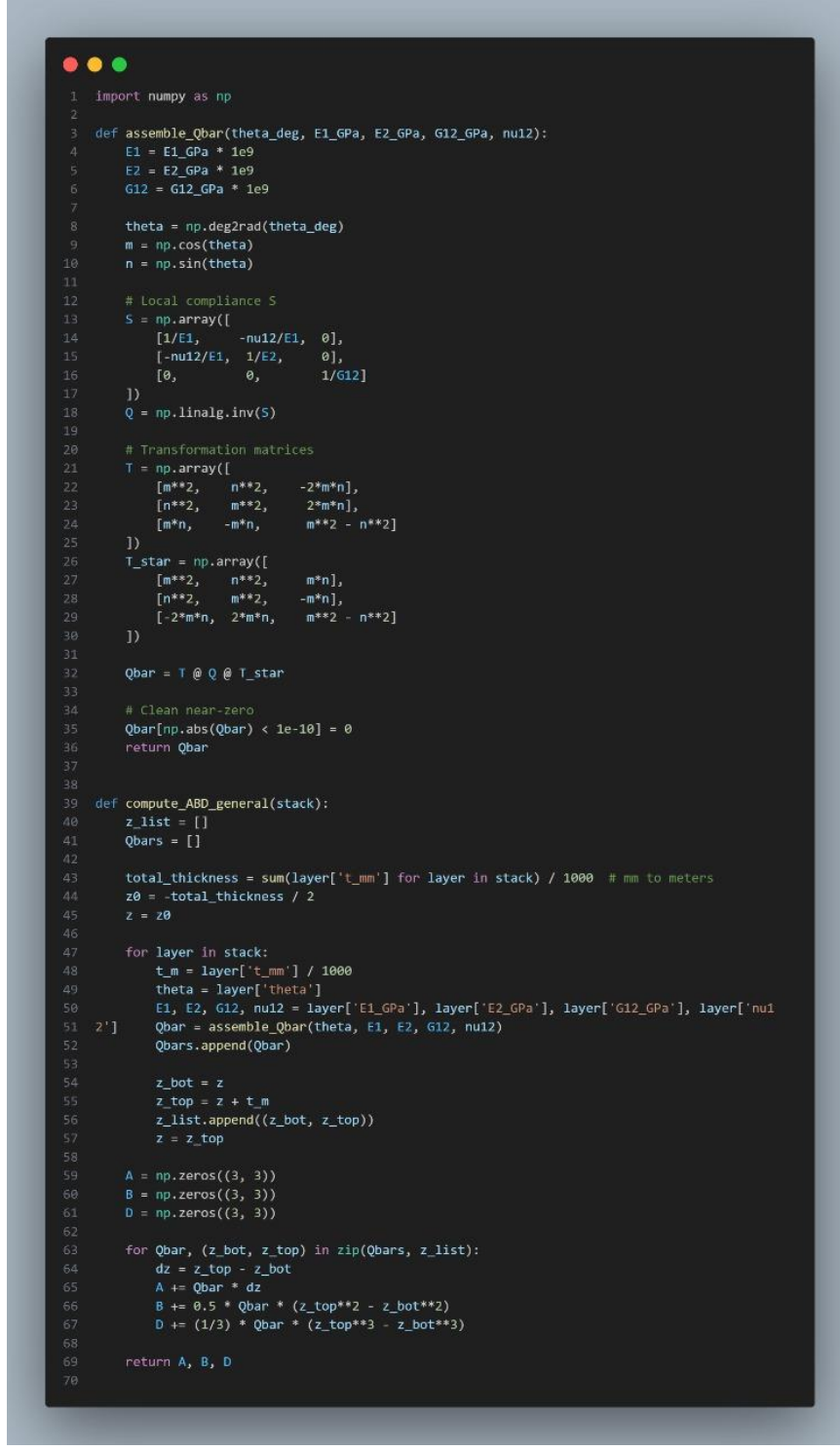
## 11. REFERENCES

1. <https://jpscm.com/products/e-glass-s-glass/>
2. <https://www.smicomposites.com/comparing-e-glass-vs-s-glass-key-differences-and-benefits/>
3. <https://www.compositesone.com/product/advanced-reinforcements/s-glass/>
4. <https://www.hitex-composite.com/products/S-Glass-Fabric.html>
5. <https://www.agy.com/aerospace-2/>
6. <https://vectorply.com/reinforcement-fibers/>
7. <https://www.wehausa.com/s-type-fiberglass-s/2655.html>
8. <https://www.dupont.com/fabrics-fibers-and-nonwovens/nomex-for-aerospace.html>
9. <https://www.dupont.com/fabrics-fibers-and-nonwovens/kevlar-for-aerospace.html>
10. <https://cacomposites.com/core-materials/kevlar-honeycomb-cores/>
11. <https://axiommaterials.com/products/aerospace-grade-nomex-honeycomb/>
12. [https://www.toraytac.com/media/5527e573-2e72-4aa4-bda7-5a49a20fef06/guunTA/TAC/Documents/Data\\_sheets/Adhesives\\_and\\_Core/Honeycomb\\_core/Nomex-Honeycomb-Core-Aerospace-Grade\\_PDS.pdf](https://www.toraytac.com/media/5527e573-2e72-4aa4-bda7-5a49a20fef06/guunTA/TAC/Documents/Data_sheets/Adhesives_and_Core/Honeycomb_core/Nomex-Honeycomb-Core-Aerospace-Grade_PDS.pdf)
13. <https://compositeenvisions.com/document/resin-selection/>
14. <https://exelcomposites.com/guide-to-composites/resin-choices/>
15. <https://fiberglasswarehouse.com/blogs/news/ultimate-fiberglass-and-resin-guidebook-for-beginners>
16. <https://smaritechonline.com/resources/blog/vacuum-bagging-advantages/>
17. <https://www.addcomposites.com/post/what-is-automated-fibre-placement-afp>
18. [https://www.bpf.co.uk/plastipedia/processes/Resin\\_Transfer\\_Molding.aspx](https://www.bpf.co.uk/plastipedia/processes/Resin_Transfer_Molding.aspx)
19. <https://hawthorncomposites.com/portfolio/switching-from-carbon-fiber-prepreg-to-resin-transfer-molding>
20. <https://incomepultrusion.com/filament-winding-an-in-depth-look/>
21. <https://www.addcomposites.com/post/filament-winding>
22. [https://www.scottbader.com/knowledge-hub/composites/hand-lay-up/?sb\\_analytics\\_cookies=accept](https://www.scottbader.com/knowledge-hub/composites/hand-lay-up/?sb_analytics_cookies=accept)
23. <https://smaritechonline.com/resources/blog/vacuum-bagging-advantages/>
24. [https://www.bpf.co.uk/plastipedia/processes/Resin\\_Transfer\\_Molding.aspx](https://www.bpf.co.uk/plastipedia/processes/Resin_Transfer_Molding.aspx)
25. <https://hawthorncomposites.com/portfolio/switching-from-carbon-fiber-prepreg-to-resin-transfer-molding/>

26. [https://scholarcommons.sc.edu/cgi/viewcontent.cgi?params=/context/emec\\_facpub/article/1840/&path\\_info=1\\_s2.0\\_S2666682021000773\\_main.pdf](https://scholarcommons.sc.edu/cgi/viewcontent.cgi?params=/context/emec_facpub/article/1840/&path_info=1_s2.0_S2666682021000773_main.pdf)
27. <https://incomepultrusion.com/filament-winding-an-in-depth-look/>
28. <https://ntrs.nasa.gov/api/citations/19880004775/downloads/19880004775.pdf>
29. <https://www.jiudingmaterial.com/news/the-advantages-and-disadvantages-of-hand-lay-up/>
30. <https://protataluk.com/blog/additive-manufacturing-advantages-and-disadvantages/>
31. <https://www.learnleansigma.com/guides/decision-matrix-analysis/>
32. <https://www.nitprocomposites.com/blog/what-is-vacuum-bagging-process>
33. <https://acpcomposites.com/category/vacuum-bagging>
34. <https://www.fibreglast.com/blogs/learning-center/vacuum-bagging-equipment-techniques-for-room-temp-applications>
35. <https://smartechonline.com/resources/blog/vacuum-bagging-advantages/>
36. <https://www.compositesworld.com/articles/avoiding-the-pitfalls-of-vacuum-infusion-processing>
37. <https://incomepultrusion.com/vacuum-infusion-a-comprehensive-guide/>
38. <https://smartechonline.com/resources/blog/vacuum-bagging-advantages/>
39. <https://www.compositesworld.com/articles/avoiding-the-pitfalls-of-vacuum-infusion-processing>
40. Kassapoglou, C., "Minimum Cost and Weight Design of Fuselage Frames Part A: Design Constraints and Manufacturing Process Characteristics."
41. Caminero, M. A., Rodríguez, G. P., and Muñoz, V., "Effect of Stacking Sequence on Charpy Impact and Flexural Damage Behavior of Composite Laminates," *Composite Structures*, Vol. 136, 2016, pp. 345–357. <https://doi.org/10.1016/j.compstruct.2015.10.019>
42. Vasudevan, A., Pandiyarajan, R., Navin Kumar, B., and Vijayarangam, J., "Effect of Kevlar Ply Orientation on Mechanical Characterization of Kevlar-Glass Fiber Laminated Composites," Vol. 988, 2020. <https://doi.org/10.1088/1757-899X/988/1/012088>
43. Mujahid, Y., Sallih, N., Mustapha, M., Abdullah, M. Z., & Mustapha, F. (2020). Effects of processing parameters for vacuum-bagging-only method on shape conformation of laminated composites. *Processes*, 8(9). <https://doi.org/10.3390/PR8091147>
44. Xuijie Zhu, Chao Xiong, Junhui Yin, Huanran Zhou, Huiyong Deng, Youchun Zou, Bending responses of CFRP thin-walled tubes with different sectional shapes: Experimental, analytical and numerical investigation, *Composite Structures*, Volume 304, Part 1, 2023, 116374, ISSN 0263-8223, <https://doi.org/10.1016/j.compstruct.2022.116374>.
45. [Lamination Parameters for Sandwich and Hybrid Material Composites](#), Gustavo H. C. Silva and Yasser Meddaikar, AIAA Journal 2020 58:10, 4604-4611
46. Harris, Charles & Shuart, M. & Starnes, James. (2002). Design and Manufacturing of Aerospace Composite Structures, State-of-the-Art Assessment. *Journal of Aircraft - J AIRCRAFT*. 39. 545-560. 10.2514/2.2992.
47. Parvez, Bisma & Kittur, Mohammed Ibrahim & Badruddin, Irfan & Kamangar, Sarfaraz & Hussien, Mohamed & Umarfarooq, M A. (2022). Scientific Advancements in Composite Materials for Aircraft Applications: A Review. *Polymers*. 14. 5007. 10.3390/polym14225007.

48. Kaufman, Brett & Briant, Clyde. (2018). Metallurgical Design and Industry Prehistory to the Space Age: Prehistory to the Space Age. 10.1007/978-3-319-93755-7, Page 285
49. <https://ntrs.nasa.gov/api/citations/19970017924/downloads/19970017924.pdf>, Accessed 27/03/2025

## APPENDIX



```

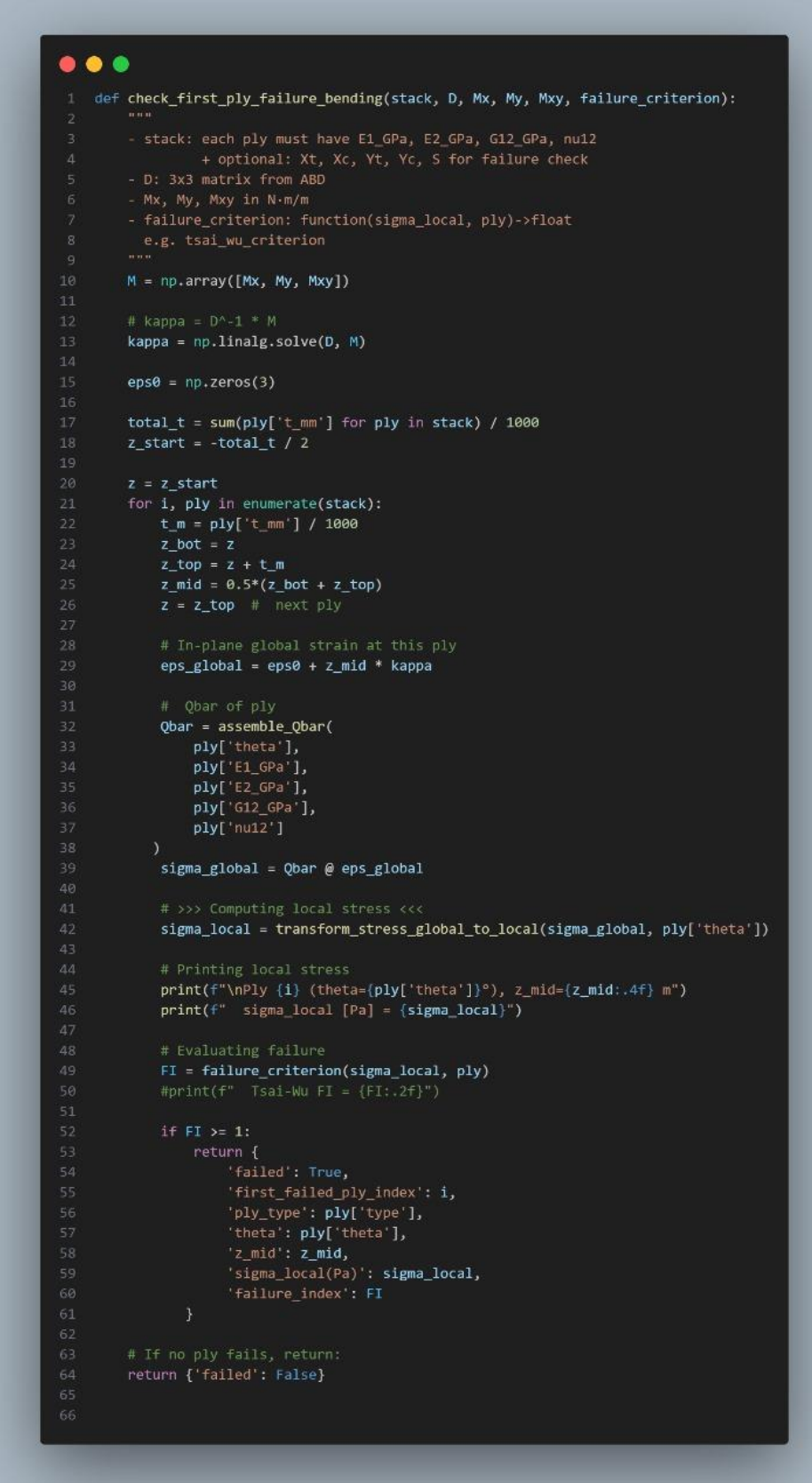
1 import numpy as np
2
3 def assemble_Qbar(theta_deg, E1_GPa, E2_GPa, G12_GPa, nu12):
4     E1 = E1_GPa * 1e9
5     E2 = E2_GPa * 1e9
6     G12 = G12_GPa * 1e9
7
8     theta = np.deg2rad(theta_deg)
9     m = np.cos(theta)
10    n = np.sin(theta)
11
12    # Local compliance S
13    S = np.array([
14        [1/E1, -nu12/E1, 0],
15        [-nu12/E1, 1/E2, 0],
16        [0, 0, 1/G12]
17    ])
18    Q = np.linalg.inv(S)
19
20    # Transformation matrices
21    T = np.array([
22        [m**2, n**2, -2*m*n],
23        [n**2, m**2, 2*m*n],
24        [m*n, -m*n, m**2 - n**2]
25    ])
26    T_star = np.array([
27        [m**2, n**2, m*n],
28        [n**2, m**2, -m*n],
29        [-2*m*n, 2*m*n, m**2 - n**2]
30    ])
31
32    Qbar = T @ Q @ T_star
33
34    # Clean near-zero
35    Qbar[np.abs(Qbar) < 1e-10] = 0
36    return Qbar
37
38
39 def compute_ABD_general(stack):
40     z_list = []
41     Qbars = []
42
43     total_thickness = sum(layer['t_mm'] for layer in stack) / 1000 # mm to meters
44     z0 = -total_thickness / 2
45     z = z0
46
47     for layer in stack:
48         t_m = layer['t_mm'] / 1000
49         theta = layer['theta']
50         E1, E2, G12, nu12 = layer['E1_GPa'], layer['E2_GPa'], layer['G12_GPa'], layer['nu12']
51         Qbar = assemble_Qbar(theta, E1, E2, G12, nu12)
52         Qbars.append(Qbar)
53
54         z_bot = z
55         z_top = z + t_m
56         z_list.append((z_bot, z_top))
57         z = z_top
58
59         A = np.zeros((3, 3))
60         B = np.zeros((3, 3))
61         D = np.zeros((3, 3))
62
63         for Qbar, (z_bot, z_top) in zip(Qbars, z_list):
64             dz = z_top - z_bot
65             A += Qbar * dz
66             B += 0.5 * Qbar * (z_top**2 - z_bot**2)
67             D += (1/3) * Qbar * (z_top**3 - z_bot**3)
68
69     return A, B, D
70

```

```

1 def transform_stress_global_to_local(sigma_global, theta_deg):
2     """
3         sigma_global = [sigma_x, sigma_y, tau_xy]
4         return [sigma_1, sigma_2, tau_12] in local (1-2) fiber coords
5     """
6     theta = np.deg2rad(theta_deg)
7     m = np.cos(theta)
8     n = np.sin(theta)
9
10    T_sigma = np.array([
11        [m**2,   n**2,   2*m*n],
12        [n**2,   m**2,   -2*m*n],
13        [-m*n,   m*n,   m**2 - n**2]
14    ])
15    return T_sigma @ sigma_global
16
17
18 def tsai_wu_criterion(sigma_local, ply):
19     """
20         sigma_local = [sigma1, sigma2, tau12]
21         ply needs 'Xt', 'Xc', 'Yt', 'Yc', 'S' in Pascals
22         returns failure index (>-1 => fail)
23     """
24     sigma1, sigma2, tau12 = sigma_local
25
26     Xt = ply.get('Xt', 1)
27     Xc = ply.get('Xc', 1)
28     Yt = ply.get('Yt', 1)
29     Yc = ply.get('Yc', 1)
30     S = ply.get('S', 1)
31
32     F1 = 1/Xt - 1/Xc
33     F2 = 1/Yt - 1/Yc
34     F11 = 1/(Xt * Xc)
35     F22 = 1/(Yt * Yc)
36     F66 = 1/(S**2)
37     F12 = -0.5 / np.sqrt(Xt * Xc * Yt * Yc)
38
39     FI = (F1*sigma1 + F2*sigma2
40           + F11*sigma1**2 + F22*sigma2**2
41           + F66*tau12**2
42           + 2*F12*sigma1*sigma2)
43     return FI
44
45
46 def check_first_ply_failure_bending(stack, D, Mx, My, Mxy, failure_criterion):
47     """
48         - stack: each ply must have E1_GPa, E2_GPa, G12_GPa, null2
49             + optional: Xt, Xc, Yt, Yc, S for failure check
50         - D: 3x3 matrix from ABD
51         - Mx, My, Mxy in N-mm
52         - failure_criterion: function(sigma_local, ply)->float
53             e.g. tsai_wu_criterion
54     """
55     M = np.array([Mx, My, Mxy])
56
57     # kappa = D^-1 * M
58     kappa = np.linalg.solve(D, M)
59
60     eps0 = np.zeros(3)
61
62     total_t = sum(ply['t_mm'] for ply in stack) / 1000
63     z_start = -total_t / 2
64
65     z = z_start
66     for i, ply in enumerate(stack):
67         t_m = ply['t_mm'] / 1000
68         z_bot = z
69         z_top = z + t_m
70         z_mid = 0.5*(z_bot + z_top)
71         z = z_top # next ply
72
73         # In-plane global strain at this ply
74         eps_global = eps0 + z_mid * kappa
75
76         # Qbar of ply
77         Qbar = assemble_Qbar(
78             ply['theta'],
79             ply['E1_GPa'],
80             ply['E2_GPa'])

```



```

1 def check_first_ply_failure_bending(stack, D, Mx, My, Mxy, failure_criterion):
2     """
3         - stack: each ply must have E1_GPa, E2_GPa, G12_GPa, nu12
4             + optional: Xt, Xc, Yt, Yc, S for failure check
5         - D: 3x3 matrix from ABD
6         - Mx, My, Mxy in N·m/m
7         - failure_criterion: function(sigma_local, ply)->float
8             e.g. tsai_wu_criterion
9     """
10    M = np.array([Mx, My, Mxy])
11
12    # kappa = D^-1 * M
13    kappa = np.linalg.solve(D, M)
14
15    eps0 = np.zeros(3)
16
17    total_t = sum(ply['t_mm'] for ply in stack) / 1000
18    z_start = -total_t / 2
19
20    z = z_start
21    for i, ply in enumerate(stack):
22        t_m = ply['t_mm'] / 1000
23        z_bot = z
24        z_top = z + t_m
25        z_mid = 0.5*(z_bot + z_top)
26        z = z_top # next ply
27
28        # In-plane global strain at this ply
29        eps_global = eps0 + z_mid * kappa
30
31        # Qbar of ply
32        Qbar = assemble_Qbar(
33            ply['theta'],
34            ply['E1_GPa'],
35            ply['E2_GPa'],
36            ply['G12_GPa'],
37            ply['nu12']
38        )
39        sigma_global = Qbar @ eps_global
40
41        # >>> Computing local stress <<<
42        sigma_local = transform_stress_global_to_local(sigma_global, ply['theta'])
43
44        # Printing local stress
45        print(f"\nPly {i} (theta={ply['theta']}°), z_mid={z_mid:.4f} m")
46        print(f" sigma_local [Pa] = {sigma_local}")
47
48        # Evaluating failure
49        FI = failure_criterion(sigma_local, ply)
50        #print(f" Tsai-Wu FI = {FI:.2f}")
51
52        if FI >= 1:
53            return {
54                'failed': True,
55                'first_failed_ply_index': i,
56                'ply_type': ply['type'],
57                'theta': ply['theta'],
58                'z_mid': z_mid,
59                'sigma_local(Pa)': sigma_local,
60                'failure_index': FI
61            }
62
63    # If no ply fails, return:
64    return {'failed': False}
65
66

```

```

1  if __name__ == "__main__":
2      stack = [
3          {'type': 'laminate', 'theta': 0, 't_mm': 0.2, 'E1_GPa': 45, 'E2_GPa': 11, 'G12_GPa': 4.5, 'nu12': 0.29},
4          {'type': 'laminate', 'theta': 45, 't_mm': 0.2, 'E1_GPa': 45, 'E2_GPa': 11, 'G12_GPa': 4.5, 'nu12': 0.29},
5          {'type': 'laminate', 'theta': 90, 't_mm': 0.2, 'E1_GPa': 45, 'E2_GPa': 11, 'G12_GPa': 4.5, 'nu12': 0.29},
6          {'type': 'laminate', 'theta': 45, 't_mm': 0.2, 'E1_GPa': 45, 'E2_GPa': 11, 'G12_GPa': 4.5, 'nu12': 0.29},
7          {'type': 'core', 'theta': 0, 't_mm': 3.2, 'E1_GPa': 0.2, 'E2_GPa': 0.2, 'G12_GPa': 0.05, 'nu12': 0.33},
8          {'type': 'laminate', 'theta': 45, 't_mm': 0.2, 'E1_GPa': 45, 'E2_GPa': 11, 'G12_GPa': 4.5, 'nu12': 0.29},
9          {'type': 'laminate', 'theta': 90, 't_mm': 0.2, 'E1_GPa': 45, 'E2_GPa': 11, 'G12_GPa': 4.5, 'nu12': 0.29},
10         {'type': 'laminate', 'theta': 45, 't_mm': 0.2, 'E1_GPa': 45, 'E2_GPa': 11, 'G12_GPa': 4.5, 'nu12': 0.29},
11         {'type': 'laminate', 'theta': 0, 't_mm': 0.2, 'E1_GPa': 45, 'E2_GPa': 11, 'G12_GPa': 4.5, 'nu12': 0.29},
12     ]
13
14     # Example strengths for the laminate plies
15     default_lam_strengths = {
16         'Xt': 1725e6, # 1725 MPa in Pa
17         'Xc': -690e6, # 690 MPa
18         'Yt': 49e6, # 49 MPa
19         'Yc': -158e6, # 158 MPa
20         'S': 70e6 # 70 MPa
21     }
22     # Attach strengths to laminate plies only
23     for ply in stack:
24         if ply['type'] != 'core':
25             ply.update(default_lam_strengths)
26
27     # Compute ABD
28     A, B, D = compute_ABD_general(stack)
29     print("A Matrix (N/m):\n", np.round(A, 2))
30     print("\nB Matrix (N):\n", np.round(B, 2))
31     print("\nD Matrix (N·m):\n", np.round(D, 2))
32
33     # Apply a bending moment
34     Mx_test, My_test, Mxy_test = 649662.531, 0, 0 # N·m/m
35     result = check_first_ply_failure_bending(
36         stack, D,
37         Mx=Mx_test, My=My_test, Mxy=Mxy_test,
38         failure_criterion=tsai_wu_criterion
39     )
40
41     if result['failed']:
42         print("\nFirst Ply Failure Detected!")
43         print(result)
44     else:
45         print("\nNo ply has failed under the given bending moment.")
46

```